Another fundamental issue is the proper discriminating measure when two systems are under consideration. In classical information theory, one employs the Kullback – Leibler relative entropy for this purpose which also has its quantum version. These are also additive measures and the Tsallis counterparts of these have been put forward and employed in the quantum context as well [10, 11]. There is promise in future work using the Tsallis approach to problems arising in quantum information theory, especially in the areas of quantum algorithms and quantum computing.

There has been some discussion of the thermodynamics of information, in particular quantum information. Since there are hints that quantum entanglement may not be additive, and since the concept of entropy has been introduced into the discussion, an examination of maximum Tsallis entropy subject to constraints such as the Bell-Clauser- Horne-Shimony-Holt observable was studied for purposes of inferring quantum entanglement [5, 6].

Acknowledgements

AKR and RWR are supported in part by the US Office of Naval Research and AKR by the Air Force Research Laboratory, Rome, New York.

About the authors

A.K. Rajagopal obtained his Master's degree from the Indian Institute of Science, Bangalore, India and a Doctor's degree from Harvard University, Massachusetts, USA. In the past twenty years he has been a Research Physicist at the Naval Research Laboratory, Washington D. C. Recently the focus of his work has been in Statistical Mechanics and Quantum Information.

R. W. Rendell obtained a PhD in Physics from the University of California at Santa Barbara. For the past twenty years he has been a Research Physicist at the Naval Research Laboratory, Washington D.C. Recently the focus of his work has been in Nanoscience and Quantum Information.

References

[1] A. K. Rajagopal in *Lecture Notes in Physics,* (eds. Sumiyoshi Abe and Yuko Okamoto) Springer-Verlag, New York (2001) gives an account of Tsallis entropy as a unified basis of both quantum statistical mechanics of many-particle systems as well as quantum information. (Lecture series were held during February 15-19, 1999)

[2] M. Gell-Mann and C. Tsallis (eds.) *Nonextensive Entropy – Interdisciplinary Applications,* Oxford Univ. Press, New York (2004); *Physica D* **193**, (2004), Special Issue on Anomalous Distributions, Nonlinear Dynamics and Nonextensivity, edited by H. Swinney and C. Tsallis.

[3] M. A. Nielsen and L.L. Chuang, *Quantum Computation and Quantum Information,* Cambridge Univ. Press, Cambridge (2000)

[4] P. W. Shor, *Commun. Math. Phys.* **246,** 453 (2004)

[5] A. K. Rajagopal, *Phys. Rev. A* **60**, 4338 (1999)

[6] S. Abe and A. K. Rajagopal, *Phys. Rev. A* **60**, 3461 (1999)

[7] A. K. Rajagopal and S. Abe, *Phys. Rev. Lett.* **83**, 1711 (1999)

[8] S. Abe and A. K. Rajagopal, *Physica. A* **289**, 157 (2001); C. Lloyd, and M. Baranger, *Phys. Rev. A* **63**, 042103 (2001); S. Abe, *Phys. Rev. A* **65**, 052323 (2002)

[9] A. K. Rajagopal and R. W. Rendell, *Phys. Rev. A* **66**, 022104 (2002)

[10] S. Abe, *Phys. Rev. A* **68**, 032302 (2003)

[11] S. Abe and A.K. Rajagopal, *Phys. Rev. Lett.* **91**, 120601 (2001)

Entropy and statistical complexity in brain activity

A. Plastino [1,2] and O.A. Rosso [3,4]
[1] Departament de Fisica. Universitat de les Illes Balears. E-070701 Palma de Mallorca, Spain;
*[2] Facultad de Ciencias Exactas and Instituto de Física La Plata Universidad Nacional de La Plata and CONICET, Argentina. C.C. 727, 1900 La Plata, Argentina **
[3] Institut für Mathematik, Universität zu Lübeck, Wallstrasse 40, D-23538 Lübeck, Germany
*[4] Instituto de Cálculo, Facultad de Ciencias Exactas y Naturales, Universidad de Buenos Aires. Pabellón II, Ciudad Universitaria. 1428 Buenos Aires, Argentina. **
** Permanent address*

Electroencephalograms (EEG) are brain-signals that provide us with information about the mean brain electrical activity, as measured at different sites of the head. EEGs not only provide insight concerning important characteristics of the brain activity but also yield clues regarding the underlying associated neural dynamics. The processing of information by the brain is reflected in dynamical changes in this electrical activity. The ensuing activity-variations are found in (*i*) time, (*ii*) frequency, and (*iii*) space. It is then very important to have theoretical tools able to describe qualitative and quantitative variations of these brain-signals in both time and frequency. Epileptic signals (ES) are specially important sources of brain information. We concentrate on ES in this article. The EEG-signal is what mathematicians call a non stationary time-series (ST). Powerful analytical methods have been developed over the years to extract information from ST. The brain ST is contaminated by another body-signals (called artifacts) due mainly to eye movements and muscle activity. Artifacts related to muscle contractions are specially troublesome in the case of epileptic seizures that exhibit rigidity and convulsions (called tonic-clonic seizures). The troublesome artifacts acquire here very high amplitudes that contaminate the whole recording. A drastic way of preventing this contamination is by injecting curare to the patient. The classic work of this type is that of Gastaut and Boughton (GAB) [1], who described the characteristic frequency pattern of a tonic-clonic epileptic seizure (ACES) in patients subjected to muscle relaxation from curarization and artificial respiration. They found that, after a short period characterized by phase desynchronization of the brain' signals, a typical feature appears in the records, baptized by them as an "epileptic recruiting rhythm" (ERR, at about 10 *Hz*). Later, as the seizure ends, they detected a progressive increase of lower frequencies associated with the convulsive phase. The TCES proceeds as follows: about 10 *s* after seizure onset, lower frequencies (0.5-3.5 *Hz*) are observed that gradually diminish their activity. The convulsive activity is associated to generalized polyspike bursts from muscle-jerks. Very slow irregular activity dominates then the EEG, accompanied with a gradual frequency increase of up to (3.5 - 12.5 *Hz*), indicative of the end of the seizure.

In Fig. 1.a we depict a typical EEG signal (sample frequency $\omega_s = 102.4$ *Hz*, for signal acquisition details see Ref. [2]) corre-

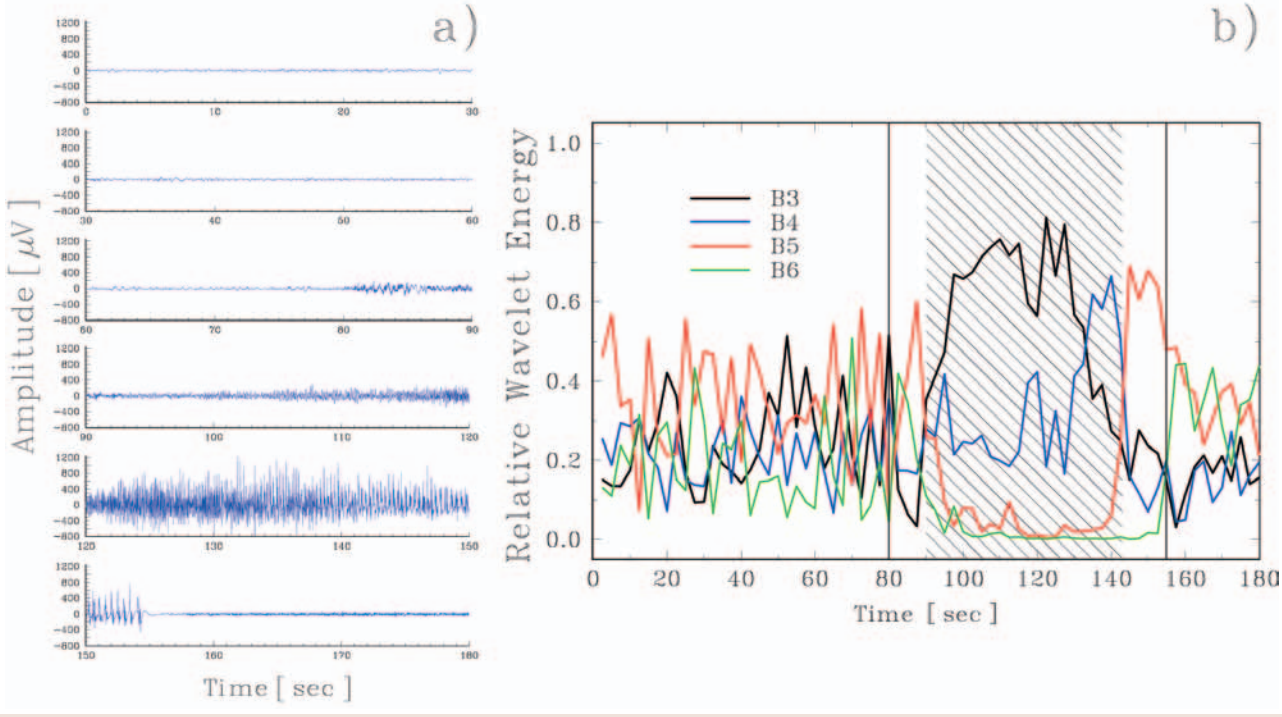

▲ **Fig. 1:** *a)* EEG signal for a tonic-clonic epileptic seizure. The seizure starts at 80 *s* and the clonic phase at 125 *s*. The seizure ends at 155 *s*. Notice that, visually, the dramatic transition from rigidity (tonic stage) to convulsions (clonic stage) around 125 *s* is not clearly discernible. *b)* Time-evolution of the relative wavelet energy corresponding to EEG noise-free signal (without contribution of frequency bands B_1 and B_2, representing frequency contributions > 12.8 *Hz* corresponding mainly to muscular activity that blur the EEG signal). From this figure it is clear that the seizure is dominated by the middle frequency bands B_3 and B_4 (12.8 - 3.2 *Hz*), with a corresponding abrupt activity decreases in the low frequency bands B_6 and B_6 (3.2 - 0.8 *Hz*). This behavior can be associated with the "epileptic recruiting rhythm" - 10 *Hz* (shadowed area in the figure). The vertical lines represent the start and the ending of the epileptic seizure.

sponding to a TCES. Recordings were performed under video control in order to have an accurate determination of the different stages of the seizure. The seizure starts at 80 *s*, with a "discharge" of slow waves superposed by fast ones with lower amplitude. This discharge lasts approximately 8 *s* and has a mean amplitude of 100 μV. Afterwards, the seizure spreads, making the analysis of the EEG more difficult due to muscle artifacts. However, it is possible to establish the beginning of the convulsive phase at around 125 *s*, and the end of the seizure at 155 *s*, where there is an abrupt decay of the signal's amplitude. Notice that it is almost impossible to visually detect the rigidity-to-convulsions (tonic-clonic) transition.

In the mathematical characterization of these brain electrical signals, that one regards as a time-series, we follow what is called a "Wavelet Transform – Information Theory" approach that is able to extract information form signals like that of Fig. 1. The basic elements of the Math we used are called wavelet transform coefficients that we derive from the EEG signal. It was our main idea that of associating a probability distribution (PD) to this time series. If one is in possession of a PD, then the branch of mathematics called Information Theory allows one to evaluate specific quantities, called quantifiers, that contain otherwise inaccessible information. Thus we go from the "bare"-signal of Fig. 1 to quantifiers that can tell us a lot about the EEG. We devised three quantifiers for EEG analysis. For computing these quantifiers we use another Math tool called "wavelet analysis". This is a method which expresses the original signal in terms of what is called a basis of an space of functions. Wavelets are just an appropriate basis, of elements here called $\psi_{j,k}(t)$, and allow for characterizing the signal by the amplitude-distribution in such a basis [3]. The wavelet coefficients represent the elements $C_j(k)$ of this distribution and efficiently provide both full information and a direct estimation of signal-energies at different frequencies. The brain-signal under analysis is given by sampled-values $\mathcal{S} = \{s_n, n = 1, \ldots, M\}$ collected using a uniform time grid. The wavelet-expansion is carried out over all pertinent frequency-resolution levels (denoted by an index j) and writen as $\mathcal{S}(t) = \sum_{j=-N}^{-1} \sum_k C_j(k)\ \psi_{j,k}(t)$, with $N = \log_2(M)$. The wavelet coefficient series $\{C_j(k)\}$ can be interpreted as the local residual errors between successive signal-approximations at scales j and $j + 1$. It contains information on the signal $\mathcal{S}(t)$ corresponding to the frequencies $2^{j-1}\omega_s \le |\omega| \le 2^j\omega_s$.

Since the family $\{\psi_{j,k}(t)\}$ is an orthonormal basis for the space of functions, the concept of energy is linked with the usual notions derived from Fourier's theory for such spaces. The wavelet coefficients are given by $C_j(k) = <\mathcal{S}, \psi_{j,k}>$ and the signal-energy, at each resolution level $j = -1, \ldots, -N$, will be $\mathcal{E}_j = \sum_k |C_j(k)|^2$. The total signal-energy can be obtained in the fashion $\mathcal{E}_{tot} = \sum_{j<0} \mathcal{E}_j$. Finally, we define the normalized ρ_j-values, which represent the *Relative Wavelet Energy* (RWE), $\rho_j = \mathcal{E}_j/\mathcal{E}_{tot}$. This RWE is our *first quantifier*. We decided to regard these ρ_j, at different scales, as a probability distribution for the energy. Clearly, $\sum_j \rho_j = 1$ and the distribution $P = \{\rho_j\}$ can be considered as a time-scale energy probability density that constitutes a convenient tool for detecting and characterizing specific phenomena in both the time and frequency planes [2, 4, 5].

Information theory introduces tools, called entropic information measures, that provide useful criteria for analyzing and comparing different probability distributions. In looking for degrees of "disorder" in our brain-signal, we devised a math-tool, our *second quantifier,* that we call a Generalized Escort-Tsallis Entropy (GWS) [4]. It is written as

$$H_q^{(G)}[P] = \frac{1}{(q-1)} \left\{ 1 - \left[\sum_{j=-N}^{-1} (\rho_j)^{1/q} \right]^{-q} \right\} \Big/ S_q^{max} \quad (1)$$

S_q^{max} is a normalization constant that enforces the convenient inequalities $0 \le H_q^{(G)} \le 1$, that simplify the analysis to be performed.

The GWS is a measure of the degree of order/disorder of the signal and thus yields useful information concerning the underlying dynamical brain-process associated with the signal. Indeed, a very ordered process can be represented by a periodic mono-frequency signal (signal with a narrow band spectrum). A wavelet representation of such a signal will be resolved at just one unique wavelet resolution level *j*, i.e., all relative wavelet energies will be (almost) zero except at the wavelet resolution level *j* which includes the representative signal's frequency. For this special level, the relative wavelet energy will be (in our chosen energy units) almost equal to unity. As a consequence, the GWS will acquire a very small, vanishing value. A signal generated by a totally random or chaotic process can be taken as the representative of a very disordered behavior. This kind of signal will have a wavelet representation with significant contributions coming from all frequency bands. Moreover, one could expect that all contributions will be of the same order. Consequently, the relative wavelet energy will be almost equal at all resolutions levels, and the GWS will acquire its maximum possible value.

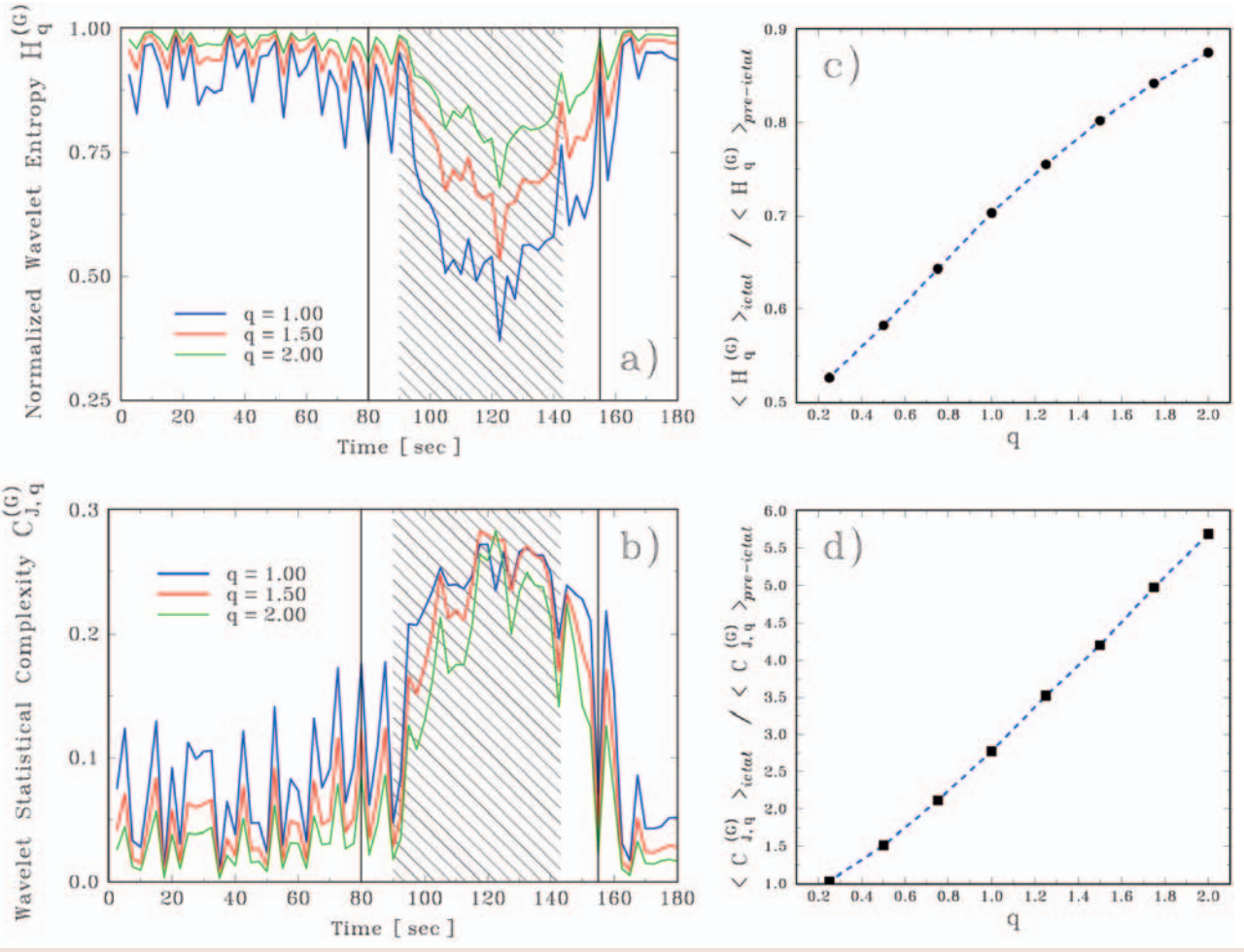

▲ **Fig. 2:** Temporal evolution of two quantifiers *a)* the normalized escort-Tsallis wavelet entropy (GWS) and *b)* Jensen escort-Tsallis wavelet statistical complexity measure (JGWC), corresponding to an EEG noise-free signal (see caption Fig. 1). The behaviour of the GWS clearly varies with *q* (see Figs. 2.a) in the temporal domain. During the pre- and post-ictal stages, these normalized GWS-values acquire a rather regular, constant behaviour, *with a dispersion that diminishes* as *q* grows. For all $q \ge 1$, the normalized GWS (JGWC) values during the ictal stage are much smaller (greater) than those pertaining to the pre-ictal stage. This difference is better appreciated in the time range corresponding to the "epileptic recruiting rhythm" (represented by a shadowed area in the figure). These features suggest that the escort-Tsallis entropy measure constitutes the appropriate tool for characterizing the tonic and clonic stages. The minimum absolute value of the normalized entropy is to be found in the vicinity of ~ 125 s, in agreement with the medical diagnosis: in that neighbourhood one encounters the tonic-clonic "phase transition". *c)* Ratio between the temporal mean value corresponding to ictal and pre-ictal epochs as function of the parameter *q* for the normalized escort-Tsallis wavelet entropy (GWS). *d)* Same for Jensen-escort-Tsallis wavelet statistical complexity measure (JGWC). This behaviour clearly illustrates the superiority of the $q > 1$ techniques that magnify differences between ictal and pre-ictal stages, critical for clinical purposes.

Ascertaining the degree of unpredictability and randomness of a system is not automatically tantamount to adequately grasping all the correlational structures that may be present, i.e., to be in a position to capture the relationship between the components of the pertinent physical system (here, the brain) [5, 6, 7]. Randomness, on the one hand, and structural correlations on the other one, are not totally independent aspects of the accompanying physical description. Certainly, the opposite extremes of perfect order and maximal randomness possess no structure to speak of (zero complexity). In between these two special instances a wide range of possible degrees of physical structure exists that should be reflected in the features of the underlying probability distribution P (here, that for the EEG). A new notion has been recently introduced in this respect, called "complexity". Complexity is a measure of off-equilibrium "order". It refers to non-equilibrium structures that arise spontaneously in certain situations. This type of "order" is not the one associated, for instance, with crystal structures, for which the entropy is very small. Biological life is a typical example of the kind of "new" order one has in mind here, associated with relatively large entropic values.

We adopt the following functional form for the "statistical complexity measure" (SCM) introduced by López-Ruiz, Mancine and Calbet [7] for a given probability distribution P:

$$C[P] = H[P] \cdot Q[P] \,, \qquad (2)$$

where Q stands for the so-called "disequilibrium" and H (defined above) represent the amount of "disorder". The quantity $Q[P] = Q_0 \cdot \mathcal{D}[P, P_e]$ is defined as a distance from the *uniform* distribution P_e among the accessible states of the system, and Q_0 is a normalization constant ($0 \le Q \le 1$). $Q[P]$ tells us just "how far" our P is located (in this space) from the uniform distribution P_e. The disequilibrium Q would reflect on the systems's "architecture", being different from zero if there exist "privileged", or "more likely" states among the accessible ones. Here we choose $\mathcal{D}[P, P_e]$ as the Jensen-escort-Tsallis divergence [8] given by

$$\mathcal{D}[P, P_e] = \frac{1}{2}\, \mathrm{K}_q^{(G)}\left[P \,\middle|\, \frac{P+P_e}{2}\right] + \frac{1}{2}\, \mathrm{K}_q^{(G)}\left[P_e \,\middle|\, \frac{P+P_e}{2}\right] \qquad (3)$$

where $\mathrm{K}_q^{(G)}[P_1|P_2]$ represent the q-Kullback escort-Tsallis entropy of P_1 with respect to P_2 (both discrete distributions) given by

$$\mathrm{K}_q^{(G)}[P_1|P_2] = \frac{1}{(q-1)} \sum_{j=1}^{N} \frac{p_j^{(1)}}{(A[P_1])^q} \cdot \left\{ \left[\frac{\left(p_j^{(2)}\right)^{1/q}}{A[P_2]} \right]^{1-q} - \left[\frac{\left(p_j^{(1)}\right)^{1/q}}{A[P_1]} \right]^{1-q} \right\} \qquad (4)$$

and $A[P] = \sum_{j=1}^{N} (p_j)^{1/q}$. The corresponding *Jensen-escort-Tsallis wavelet statistical complexity measure* (JGWC), $C_{J,q}^{(G)}$ is in this way obtained if we consider for the complexity evaluation (Eqs. (2) to (4)) that distribution P given by the RWE. The JGWC is our *third quantifier.*

For EEG-work six frequency bands are important for an appropriate wavelet analysis [3]. We denote these 6 band-resolution levels by Bj ($|j| = 1, \ldots, 6$), and proceed as follows in the evaluation of the three quantifiers that we have introduced above: RWE, GWS and JGWC, we ignore the contributions from the B_1 and B_2 bands (> 12.8 *Hz*) that contain high frequency artifacts related to muscular activity that blur the EEG [2]. Once the high frequency artifacts are eliminated, we can analyze the time evolution of the above listed three wavelet quantifiers for the "remaining" signal. For this purpose the signal is divided into epochs of lengths $L = 2.5$ *s* each ($M = 256$ *data*).

Figure 1.b displays the quantifier RWE corresponding to the EEG signal (Fig. 1.a) without contaminant artifact-contributions (B_3 to B_6). (The following, detailed description of the signal-analysis can be omitted in a first reading.) We see that the initial (called pre-ictal) phase is characterized by a dominance of low rhythms (pre-ictal: $[B_5 + B_6] \sim 50\%$). The seizure starts at 80 *s* with a discharge of slow waves superimposed on low voltage fast activity. This discharge lasts approximately 8 *s* and produces a marked "activity-rise" in the frequency bands B5 and B6, which reaches 80% of the RWE. Starting at 90 s, the low frequency activity, represented in our analysis by B_5 and B_6, decreases abruptly to relative values lower than 10%, while the other frequency bands become more important. We also observe in Fig. 1.b that the start of the convulsive (clonic) phase is correlated with increased activity in the B_4 frequency band. After 140 *s*, when clonic discharges become intermittent, the B_5 activity rises up again till the end of the seizure, when the B_6 frequency activity also increases in very rapid fashion and both frequency bands become clearly dominant. The B_5 and B_6 frequency bands maintain this predominance throughout the post-ictal phase. We conclude from this example that the seizure is dominated by the middle frequency bands B_3 and B_4 (12.8-3.2 *Hz*), with a corresponding abrupt activity decrease in the low frequency bands B_5 and B_6 (3.2-0.8 *Hz*). Clearly, this behavior can be associated with the above described epileptic recruiting rhythm (ERR) [1] (shadowed area in the figure). We emphasize the fact that our results were obtained without the use of curare or any filtering method.

The other quantifiers, GWS and JGWC, as a function of time, are depicted in Figs. 2.a and 2.b. In their evaluation we ignore contributions due to contaminant high frequency bands (B_1 and B_2). The behavior of the GWS clearly varies with q (see Figs. 2.a) in the temporal domain. During the pre- and post-crisis (ictal) stages, these normalized GWS values acquire a rather regular, constant behavior, *with a dispersion that diminishes* as the Tsallis' q grows (see Figs. 2.a and 2.c). For all $q \ge 1$, the normalized GWS values during the ictal stage are much smaller than those pertaining to the pre-ictal stage. This difference is better appreciated in the time range corresponding to the ERR (represented by a shadowed area in the figure). One may therefore suggest that the escort-Tsallis entropy measure, that we use here, constitutes the appropriate tool for characterizing the tonic and clonic stages of the epileptic crisis.

The minimum absolute value of the normalized entropy is to be found in the vicinity of ~ 125 *s*, in agreement with the medical diagnosis: in that neighbourhood one encounters the tonic-clonic "phase transition", that one can detect by looking at the patient but not by inspection of the bare record of Fig. 1. Two relative maxima are observed at ~145 s and ~ 155 *s*. As stated above, these times are associated with the ends of (*i*) the ERR and (*ii*) the epileptic seizure, respectively. Changes in the EEG series around 125 *s* (transition from tonic to clonic stage) are the result of a mechanism entirely different from the one that produces variations at 145 and 155 *s* (neuronal "fatigue", a decrease of the neuronal firing rate with preponderance of inhibition factors, is largely responsible for originating the end of the seizure).

Our JGWC-quantifier numerical results also depend upon the Tsallis' q. In fact, we see from Figs. 2.b and 2.d that the JGWS yields values *with a dispersion that diminishes* as q grows (in particular for the pre- and post-ictal periods). This behaviour can be clearly appreciated in Figs. 2.c and 2.d, where the ratio between the temporal mean values corresponding to ictal and pre-ictal epochs as function of the parameter q for GWS and JGWC is shown. That is for $q < 1$ the fluctuations in these quantifiers increase and for $q > 1$ decrease, specially in pre-ictal period. This fact (*i*) emphasizes the difference between the mean values corresponding to pre-ictal and ictal stages (increase of statistical significance); (*ii*) clearly illustrates the superiority of the $q > 1$ Tsallis-techniques that magnify such

differences, that are critical for clinical purposes. However, the mean JGWS values are significatively larger in the ictal than in the pre- and post-ictal epochs for all $q \geq 1$.

The present article described informational tools derived from the orthogonal discrete wavelet transform and their application to the analysis of brain electrical signals. The quantifier (relative wavelet energy) RWE provides information concerning the relative energy associated with different frequency bands that are to be found in the EEG and enables one to ascertain their corresponding degree of importance. Our second quantifier, normalized wavelet entropy (GWS), carries information about the degree of order/disorder associated with a multi-frequency signal response. Finally, our third quantifier, the statistical wavelet complexity (JGWC), provides us with a measure that reflects the intricate structures hidden in the brain-dynamics.

In particular, it becomes clear that the ERR behavior reported by Gastaut and Broughton [1] for generalized TCES is accurately described by the RWE quantifier. Moreover, the reported study does not require the use of curare or of digital filtering. In addition, a significant decrease in the entropy was observed in the recruitment epoch, indicating a more rhythmic and ordered behavior of the EEG signal, compatible with a dynamical process of synchronization in the brain activity. In addition the recruiting phase also exhibits larger values of statistical complexity.

It is well established that an EEG is directly proportional to the local field potential recorded by electrodes on the brain's surface. Furthermore, one single EEG electrode placed on the scalp records the aggregate electrical activity from up to 6 cm^2 of the brain surface, and hence from many millions of neurons. With such large numbers, is seems quite natural to model the neocortex as a continuous sheet of neurons (neuronal matter) whose activity varies with time. Taking into account the available results for (*i*) the chaoticity index (the largest Lyapunov exponent with stationary constraints removed) as a function of time and (*ii*) the largest Lyapunov exponent for selected portions of the EEG signal, one can confidently assert that a chaotic behavior can be associated with the whole EEG signal. This chaoticity becomes smaller during the recruiting phase [2]. As pointed out by many authors (see for instance [9]), the coexistence of chaos with ordering and increasing complexity for extended system is a manifestation of self-organization. We can thus suggest, on the basis of experimental EEG data and using appropriate statistical tools, that in the case of tonic-clonic epileptic seizures, the epileptic focus triggers a self-organized brain state characterized by both order and maximal complexity.

References

[1] H. Gastaut and R. Broughton, *Epileptic Seizures.* Charles C. Thomas, Springfield, 1972.

[2] O. A. Rosso, M. L. Mairal, *Physica A* **312** (2002) 469.

[3] S. Mallat, *A Wavelet Tour of Signal Processing,* Academic Press, San Diego, 1999.

[4] O. A. Rosso, M. T. Martin, A. Plastino. *Physica A* **313** (2002) 587.

[5] O. A. Rosso, M. T. Martin, A. Plastino. *Physica A* **320** (2003) 497.

[6] P. W. Lamberti, M. T. Martin, A. Plastino, O. A. Rosso, *Physica A* **334** (2004) 119.

[7] R. López-Ruiz, H. L. Mancini, X. Calbet. *Phys Lett A* **209** (1995) 321.

[8] P. W. Lamberti, A. P. Majtey. *Physica A* **329** (2003) 81.

[9] H. Haken, *Information and Self-Organization,* Springer–Verlag, Berlin, 2000.

Long-range memory and nonextensivity in financial markets

Lisa Borland
Evnine-Vaughan Associates, Inc., 456 Montgomery Street, Suite 800, San Francisco, CA 94104, USA
lisa@evafunds.com

Perhaps one of the most vivid and richest examples of the dynamics of a complex system at work is the behavior of financial markets. The price formation process of a publicly traded asset is clearly the product of a multitude of evasive interactions. Individuals around the globe post orders to buy or sell a particular stock at a particular price. Transactions are cleared at a certain price at a given time, either by passing through the hands of a specialist on the trading floor, or automatically on the many electronic markets which have flourished along with technological advances over the past few years (Fig. 1). Apart from fundamental properties of the company whose stock is being traded, factors such as supply and demand clearly must affect the price of stocks, as well as general trends in the particular industry in question. Stock specific events, such as mergers and acquisitions, have a big impact, as do world events, such as wars, terrorist attacks and natural disasters.

Time series of financial data exhibit highly nontrivial statistical properties. What is quite fascinating is that many of these anomalous properties appear to be universal, in the sense that they are present in a variety of different asset classes, ranging for example from commodities such as wheat or oil, to currencies and individual stocks. Furthermore they are present across the geographical borders, and can be observed among others in US, European and Japanese markets.

Finding a somewhat realistic model of price variations that can capture the spectrum of interesting statistical features inherent in real data is a challenging task, important for many real-world reasons, such as risk control, the development of trading strategies, option pricing and the pricing of credit risk to name a few. Bachelier's random walk model in 1900 was the first attempt of a mathematical model of price variations. While a century ago this Gaussian stochastic process was state-of-the-art, and indeed lies at the bottom of the celebrated Black-Scholes option pricing formalism, we now know Figure 2: The empirical distribution of daily returns from the stocks comprising the SP 100 (red) is fit very well by a q-Gaussian with $q = 1.4$ (blue). that it is way too simple to describe the properties of real data. In fact, during the past decade, there has been an increasing and widespread access to data extracted from financial markets. This includes for example every single trade and quote of all stocks traded on the New York Stock Exchange, records from various electronic markets, the entire order book data from the London stock exchange, to name just a few sources. These vast amounts of historical stock price data have helped establish a variety of so-called stylized facts [1, 2], which can be seen as statistical signatures, of financial data.

The best known stylized fact is perhaps the distributions of returns (defined as logarithmic relative price changes). On time scales ranging from minutes to weeks these have fat tails, exhibiting